

Article

Not peer-reviewed version

Fragmentation of Multiply Charged C₁₀H₈ Isomers Produced in keV Range Proton Collision

[M V Vinitha](#) , Pragma Bhatt , [C P Safvan](#) , [Sarita Vig](#) , [Umesh Kadhane](#) *

Posted Date: 31 May 2023

doi: 10.20944/preprints202305.2177.v1

Keywords: PAH; proton collision; multi-fragmentation




Preprints.org is a free multidiscipline platform providing preprint service that is dedicated to making early versions of research outputs permanently available and citable. Preprints posted at Preprints.org appear in Web of Science, Crossref, Google Scholar, Scilit, Europe PMC.

Copyright: This is an open access article distributed under the Creative Commons Attribution License which permits unrestricted use, distribution, and reproduction in any medium, provided the original work is properly cited.

Article

Fragmentation of Multiply Charged $C_{10}H_8$ Isomers Produced in keV Range Proton Collision

M V Vinitha ¹ , P Bhatt ², C P Safvan ², S Vig ³ and U R Kadhane ^{1,*}

¹ Department of Physics, Indian Institute of Space Science and Technology, Thiruvananthapuram-695 547, India

² Inter-University Accelerator Centre, Aruna Asaf Ali Marg, New Delhi-110 067, India

³ Department of Earth and Space Science, Indian Institute of Space Science and Technology, Trivandrum-695 547, India

* Correspondence: umeshk@iist.ac.in

Abstract: Fragmentation processes of multiply charged ions of $C_{10}H_8$ isomers produced in fast proton collision (velocity between 1.41 and 2.4 a.u.) is discussed in view of their fundamental molecular dynamics. Especially so in the mechanisms to produce a variety of carbon clusters from such ions. This aspect is assessed with the help of a multihit analysis of daughter ions in coincidence with elimination of H^+ and CH_n^+ ($n = 0$ to 3). The elimination of H^+ / C^+ was found to be very different from CH_3^+ loss. The loss of CH_3^+ was found to be accompanied with the formation of heavy ions like $C_9H_5^+$, $C_9H_5^{2+}$ and $C_7H_3^+$ by a cascade of momentum correlated dissociations. The most probable structures of large fragment ions in the CH_3^+ loss cascade are predicted with the help of computed electronic energy and the multihit ToF correlations of second and third hit. In addition, we report observation of super-dehydrogenation of naphthalene and azulene targets, with evidence of complete dehydrogenation in a single collision.

Keywords: PAH; proton collision; multi-fragmentation

1. Introduction

The dissociation dynamics of a variety of polycyclic aromatic hydrocarbons (PAH) has been investigated under VUV absorption or energetic charged particle collisions in several reports in the past [1–13]. Such measurements provide fundamental insight into the quantum chemistry of the organic molecules with PAHs as a convenient model system. A considerable body of this research domain has focused on the dissociation of monocations. While the measurements with monocations are often supplemented by large amount of computational efforts, investigating the dissociation dynamics of highly charged ions becomes a challenge. The excess coulomb energy stored in the di- or trication can radically change the nature of the dissociation dynamics. In addition, the complexities of the data assimilation, analysis and interpretations make the investigations on multiply charged ions relatively an uncommon endeavour.

The dissociative multiple ionization of PAHs can occur in hostile astronomical regions by a number of excitation processes such as multi-stage VUV absorption, interacting with X-rays or low energy component of cosmic ray, stellar wind proton and /or ions and other energetic particles in the interstellar medium [14–17]. The laboratory research in this domain is mainly done using Extreme UV or X-ray photon, while charged particle collisions remain less explored [17–19]. In the last two decades, the study of the upper atmosphere of the jovian planets and their moons have led to substantial understanding of how energetic charged particle radiation from the sun can play a crucial role in their atmospheric composition and evolution [20–23]. In situ measurements by Cassini Huygens mission have demonstrated the importance of 10 to 100 keV energy range of Protons in the dynamics of Titan's ionosphere [22,23]. Such interactions are known to be more efficient in producing highly charged ions and a diverse energetic secondary fragment ions (C^+ , CH_3^+ and $C_2H_2^+$ etc), which eventually can lead to extremely rich and complex atmospheric chemistry in these astronomical bodies.

Here we compare the multi-fragmentation spectra of highly charged azulene ($C_{10}H_8$) and naphthalene ($C_{10}H_8$) produced in fast proton collisions. There is little difference between the multi-fragmentation of the two isomers. We mainly focus on the emission of light fragments H^+ , C^+ and CH_3^+ . The former two channels signify violent multi-fragmentation while the latter proceeds via a common intermediate isomer, which is often ignored due to its relatively low yield compared to $C_2H_2^+$ loss channel. Complete or partial dehydrogenation events are observed under a single collision conditions.

2. Computational details

Multiply charged ions in keV range collision are produced with substantial amounts of internal energy which assists in crossing various transition state barriers involved in isomerization or dissociation processes. When an intact ion of PAH eliminates smaller neutral or ionic fragment like CH_3^+ or $C_2H_2^+$, the smaller fragment will carry a substantial amount of vibrational energy per degree of freedom and larger fragment will be produced close to the final equilibrium configuration in the ground electronic state. Therefore the ground state energies were used here as a measure to predict the most probable structure of large fragment ions. Various isomers of $C_9H_5^+$ and $C_9H_{52}^+$, the large fragment ion formed after CH_3^+ loss, were optimized using the Dunning basis set cc-pVDZ to predict the total energy. The energy of doubly and triply charged $C_{10}H_8$ isomers, which can eliminate CH_3^+ is also calculated. The nonlocal hybrid Becke three-parameter Lee-Yang-Parr functional (B3LYP) with 6-31G(d) basis, incorporated in the GAUSSIAN 09 package [24], was used for the structure calculations of $C_{10}H_8$ ions.

3. Experimental details and analysis

Proton beam of energy ranging from 50 keV to 150 keV, in steps of 25 keV was extracted from the ECR ion source facility at LEIBF, IUAC, New Delhi. These ions were made to interact with the target molecules in a time-of-flight (ToF) mass spectrometry system. The emitted electron as well as possibly neutralised projectile were separately detected using channeltron detectors, one at the opposite direction the recoil ToF tube and other at about 1.5 meter distance from the interaction region. The recoil ions were accelerated and recorded using a 40 mm active diameter position sensitive microchannel plate detector (PSD) with a delay line anode. The data was recorded in common stop multihit mode. The delayed sum of the secondary electron as well as the neutralised projectile was used as a stop signal, with a relative delay adjusted to give priority to the projectile detection. The data reported here is only for electron emission mode. The target molecules of naphthalene (nph) and azulene (az) were injected in the vacuum system using a long hypodermic needle connected to an external reservoir with a valve. The target samples were kept at room temperature and the effusion of the target vapour due to their vapour pressure at room temperature was found to be adequate to perform the experiment with an event rate of about 1 to 2 kHz. Entirely different target masses (not reported here) were used in between the two experiments and totally different supply lines were used for the two targets to avoid any cross contamination. The recorded data was filtered and cleaned on the basis of electron emission or electron capture mode as well as the for the various sum conditions on the PSD. The event record was then obtained upto 8 multihits. The event recorded was adequate upto the third hit to assess the fragmentation, as the positive counts beyond this were negligibly small. Typically, for a projectile energy of 50 keV, 76 % events were purely single hit, about 19 % purely double hit and less than 4 % were triple hit. Obviously, the exact percentage is strongly dependent on the detection efficiency which varied from about 45 % for a single carbon fragment ion to about 20 % for an intact molecular ion. A detailed analysis of intact and neutral evaporation from mono- and di- cation species has already been presented elsewhere [12]. As the detection efficiency is expected to vary considerably over the recoil-ion mass and velocity, an accurate estimation of the branching ratio is not attempted here. As the focus is on multi-fragmentation or charge separation and process,

the data corresponding to all the five projectile energies were added together during the analysis to improve the statistics for multi hit analysis.

4. Results and discussions

4.1. Normalisation process

The single ionization cross section of az and nph are the same for the studied collision energies [12] and the single hit data of two isomers are normalised to the sum of singly charged parent ions ($m/q = 128$ and 129), neutral H loss ($m/q=127$) and C_2H_2 loss ($m/q = 102$) ions from parent monocation. The normalisation procedure was so chosen due to two reasons. Firstly, because the neutral H loss contribution, although negligible, was difficult to separate from the parent peak. Secondly, it was seen that both isomers had same single ionisation cross sections, but az^+ being a high energy isomer (figure 1 in [25]), experienced higher fraction of C_2H_2 emission than nph, the details of which has been discussed in the previously reported work on monocations of these two isomers [12]. All the one dimensional (1D) spectra shown henceforth are normalised by this procedure and multiplied by an arbitrary factor of 1000 (arbitrary common factor). The two dimensional (2D) spectra are shown as counts without normalisation.

4.2. Single hit analysis

The single hit mass spectrum of az and nph after normalization are found to be similar as shown in Figure 1. The mass spectra includes only the data wherein a single ionic specie detected in a given event thus the data shown is mix of pure single ion event as well as events wherein only one of the possibly multiple ions produced is detected. One striking difference between the two mass spectrum is the 60% excess yield at m/q 102 peak (loss of neutral C_2H_2 from monocation) in the az mass spectrum. This was explained on the basis of high energy difference between singly charged az and nph in our previous work [12]. Similarly a 10 % higher ion yield is observed for $C_nH_m^+$ fragments, in the az spectrum. This may again be due to the less stable configuration of az in higher charge states as suggested in a recent work (Figure 1 in [25]. But, the peaks in the region of m/q of 98 ($C_8H_m^+$ where $0 < m < 10$) and 88 ($C_7H_m^+$, where $0 < m < 10$) have identical cross sections for the two isomers. Roughly 5 % of triply charged parent monocations are detected in case of two isomers. Overall there is little difference between the multifragmentation spectra of $C_{10}H_8$ isomers, which may be due to the lower energy difference between multiply charged isomers compared to singly charged or neutral isomers. The peak at $m/q=45$ is acetone, which was used for cleaning the target lines. The sharp peaks at $m/q=20$ and 40 are due to Ar in the background. Ar was used for mass calibration.

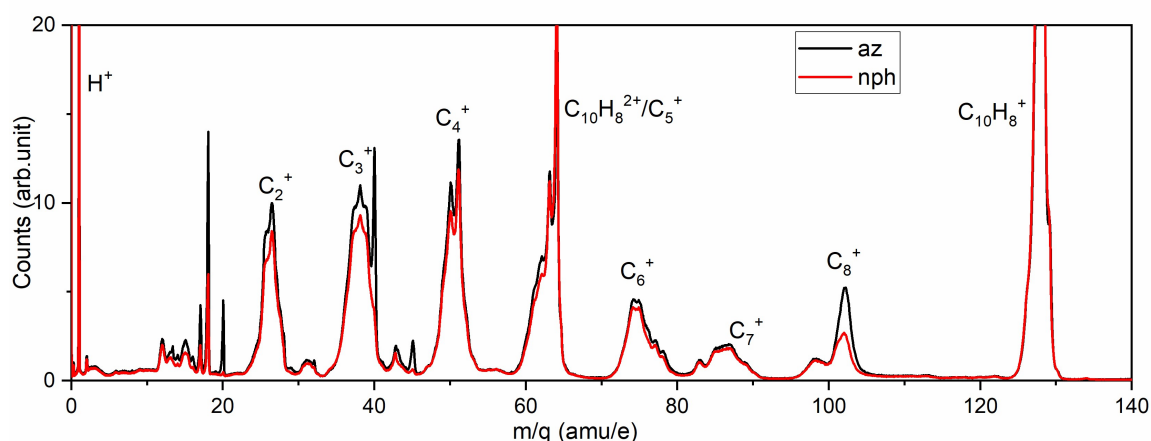


Figure 1. Normalised single hit spectrum of nph and az.

4.3. Coincidence analysis for double hit data

The use of a multi-hit time digitizer enabled the measurement of as many as eight fragments from a single event in the ToF spectrometer, provided that their flight times differed from each other by more than 10 ns. A 2D plot is made with first hit ToF on the horizontal axis and second hit ToF on the vertical axis as shown in the Figure 2. The correlation patterns are found similar for two of the isomers. The 2D correlation spectra is rich in structure with several islands, many of them are broad and have no momentum correlation. These broad islands represent multi-fragmentation/charge separation of highly charged ions, with more than two fragment ions being produced in a concerted manner. Few islands are binary fragmentation channels, which are momentum correlated and most of them have an extended tail showing a metastable fragmentation. The islands in coincidence with H^+ are the most intense channels in the 2D map. Most of the islands in the spectrum are poorly mass resolved due to high momentum release, limiting our investigation to a few sets of channels.

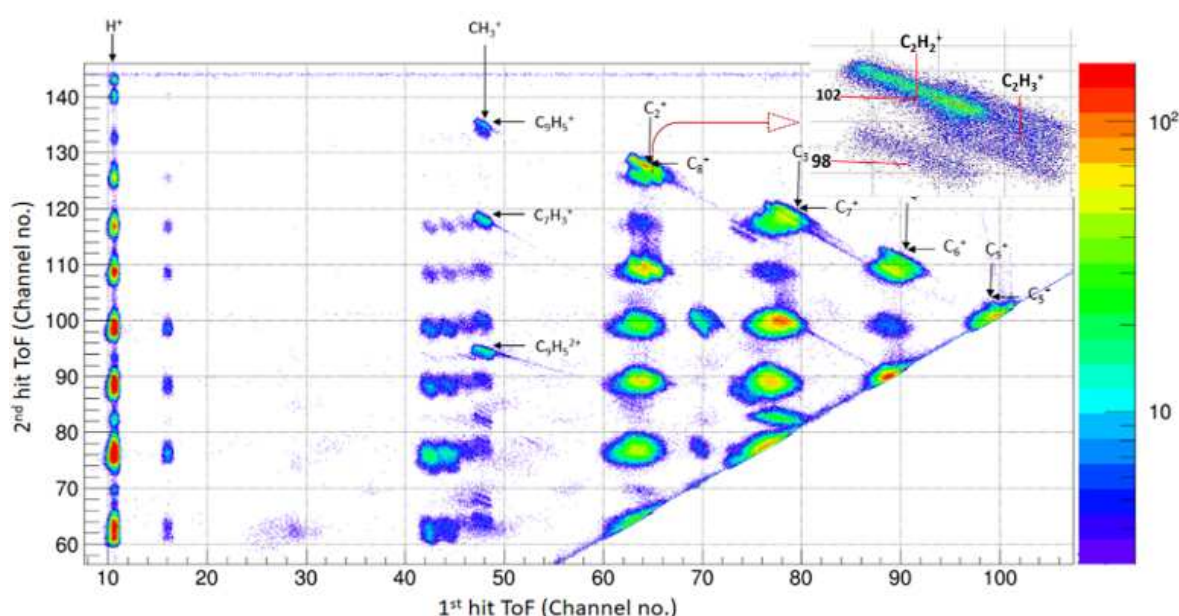
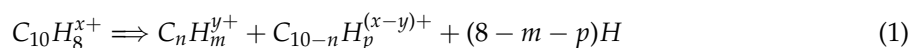


Figure 2. 1st hit vs 2nd hit ToF correlation spectrum of az (data for all projectile energy are added). The location of H^+ and CH_3^+ in the first hit is indicated at the top. Carbon conserving fragmentation channels are marked and one of them is shown in the inset.

Carbon conserving binary fragmentation channels can be summarized as below:



Among these the prominent channels are $n=8, 7$ and 6 . $n=5$ channel may also be present, but it is difficult to separate from the effect of pulse pair resolution. There are a relatively low number of events with $n=9$. Some of the channels with $n=8$ and $n=7$ have an extended tail representing a metastable or slow dissociation within the extraction time scale of ToF. Whereas all the channels in the island with $n=6$ show no tail, which indicates a fast dissociation compared to the extraction time of ToF. It appears that the heavier the fragment ion produced in a given fragmentation channel, the weaker the degree of dehydrogenation. For instance, as one goes from $n=9$ to $n=6$, the channels shift from hydrogen conserving channels to more dehydrogenated channels. In addition, there is a clear evidence of loss of H in multiples of two as observed in the previous studies [6,26]. The emission of $C_2H_2^+$ loss is one such example where the prominent H conserving channel is followed by loss of 4H or $2H_2$, but not by loss $2H/H_2$ (See the inset of Figure 2). The loss of $C_2H_3^+$, on the other hand, followed no such restriction. More such features and their details are available, but not discussed here. The violent multi-fragmentation channels can not be represented in a concise form like reaction 2, because of

the many possible combinations. Such channels are also found to have some interesting features as discussed in a few examples in the following sections.

4.4. H^+ coincidence

The single hit spectrum of nph is compared with second hit spectra in coincidence with H^+ in the first hit in the Figure 3. We detected a strong H^+ correlation with all other smaller mass fragments, which might be due to the highest detection efficiency of H^+ . Two quick observations can be made: (i) none of the peaks in the second hit spectrum are sharp. This implies that all partner fragments are produced with some kinetic energy. Also, H^+ islands have no momentum correlation in the 2D. Both of these observations indicate that H^+ originates mainly from highly charged parent ions, with charge state greater than $3+$. (ii) the intensities of fragments containing an odd number of carbon atoms, especially CH_m^+ and $C_3H_m^+$ are substantially larger than the peaks in the single hit. This is because of the oscillating binding energy of carbon clusters produced in the multi-fragmentation events [27]. The propensity of such clusters is decided by the energy of formation and the ionisation potential.

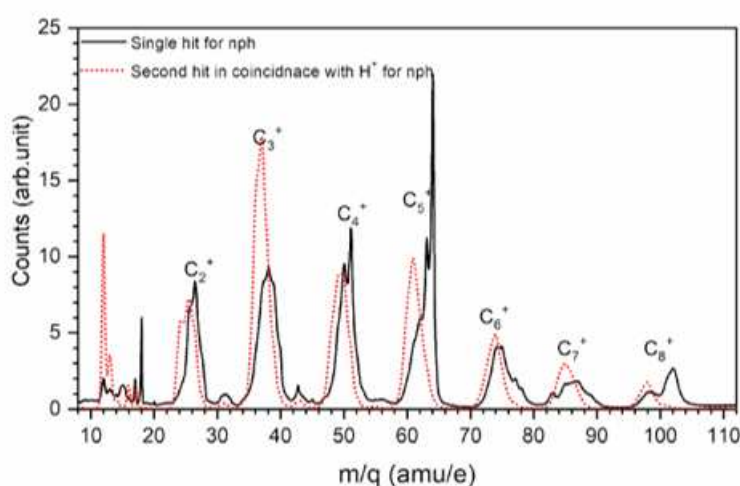


Figure 3. Comparison of single hit spectra of nph with second hit spectra in coincidence with H^+ detection in the first hit

The second hit mass spectra of az and nph obtained in coincidence with H^+ are presented in Figure 4. For the peaks around $n=6, 7$ and 8 , there is no difference between az and nph. The intensity of all other fragments are about 10% higher for az, which might be due to the inherently less stable configuration of highly charged az compared to nph. Another striking observation is the relatively small coincidence with super-dehydrogenated az or nph monocations as shown in Figure 5. For the first time, we report here the possibility of losing all hydrogen atoms from az/nph in a single collision. The system prefers to lose 2, 6, 7 or 8 hydrogens with at least one of them emitted as H^+ . Such super-dehydrogenation and the fact that the 3, 4 and 5 H loss channels are not favored require detailed investigation, which will be useful to understand the atomic and molecular hydrogen propensity in the astronomical region where PAHs are in continuous irradiation with stellar wind protons.

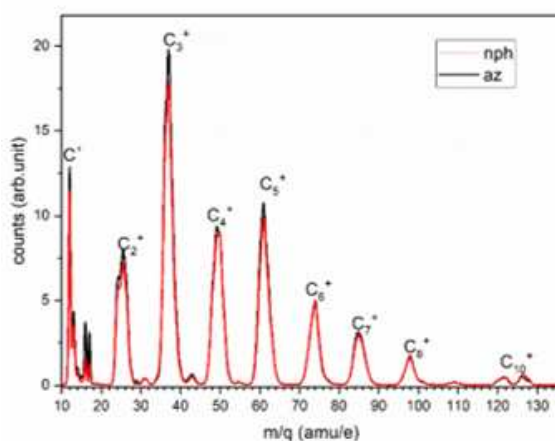


Figure 4. Second hit mass spectra of az and nph with H^+ as the first hit

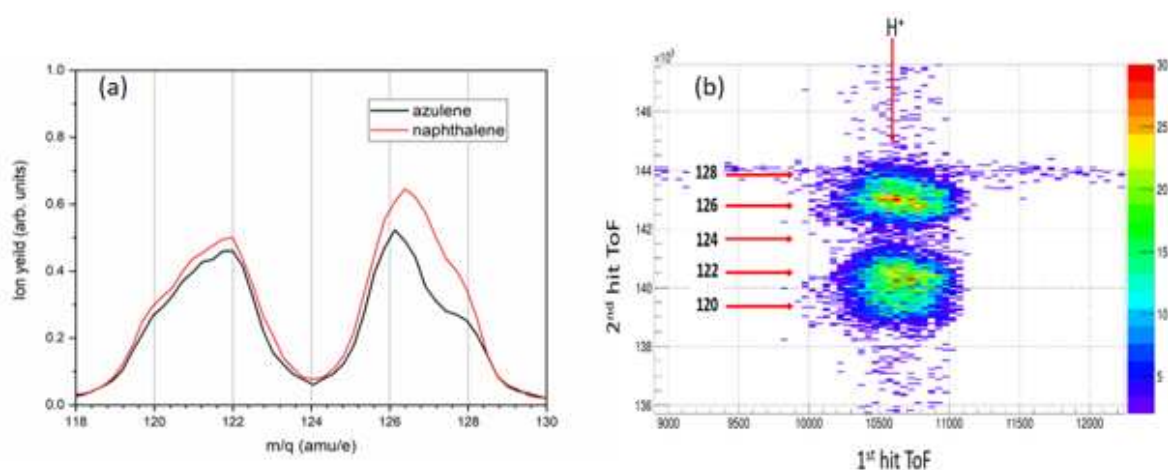


Figure 5. (a) Signature of super-dehydrogenation of az and nph, total dehydrogenation can also be noted. (b) H^+ coincidence of az in $m/q = 128$ (singly charged parent mass) region

4.5. C^+ , CH^+ , CH_2^+ coincidence

The second hit mass spectrum of az and nph in coincidence with C^+ is shown in Figure 6. The second hit mass spectra of H^+ and C^+ coincidences are similar, except that the fragment peak around $n=8$ is absent in the latter case. We also observed that the first hit fragments C^+ , CH^+ and CH_2^+ show similar second hit mass spectra with less intensity on the high mass side. The high intensity on the low mass region indicates that these fragments are also produced by multi-fragmentation of highly charged ion. The similarity between H^+ and C^+ (also CH^+ and CH_2^+) coincidence channels may also suggest that these ions are produced in a single event, but H^+ is not detected, instead C^+ is observed as the first hit event.

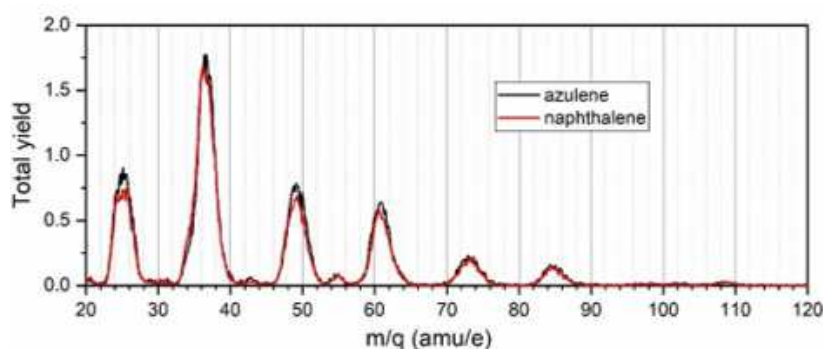


Figure 6. 2nd hit mass spectra of az and nph in coincidence with C^+

4.6. CH_3^+ Coincidence

The ring opening and ring expansion mechanisms in smaller PAHs are pivotal to the understanding of formation of larger PAHs in ISM. To this end, HACA (Hydrogen-Abstraction/acetylene-Addition) process [28] has been in the discussion for a quite some time and has been considered as a possible mechanism for the growth of larger PAHs. But, in recent years the laboratory experimental results have conclusively demonstrated that HACA mechanism is not a favourable option, since it fails to account for the possible rate of formation of PAHs in the ISM [29]. A more plausible hypothesis of ring expansion and PAH growth has been proposed by Zhao *et al.*. This mechanism involves the addition of a methyl group to the pentagon ring of a PAH so as to expand the ring to a hexagon structure and thus successively grow the size of PAHs. In this context, we looked at the second hit coincidence spectra of CH_3^+ channel and compared it with C^+ and CH^+ . In a laboratory setup, it is much easier to study the dissociation process and then try to understand the associative process, than to experimentally look for the associative reaction itself. We believe that an investigation of the parent conformers and associated reverse barriers will add significant value to the understanding of the methyl addition processes in PAHs.

The second hit mass spectrum of two isomers with CH_3^+ as the first hit are shown in Figure 7. The similarities between the two isomers are seen once again. There is a clear difference between the behaviour of the second hit mass spectrum of C^+ and CH_3^+ channels. $C_7H_3^+$, $C_9H_5^+$ and $C_9H_{52}^+$ are the major fragments formed after CH_3^+ loss. These channels appear with a tail in the 2D spectrum (2). We were able to determine the number of H atoms in each of these fragments using ToF correlations in the 2D. The mass spectrum of az below m/q of 46 was heavily contaminated by the acetone used for cleaning the target lines before introducing the az. The second hit mass spectrum of az is subtracted from nph and shown in Figure 7(b). The differential mass spectrum is dominated by fragments from acetone (below m/q of 46). We further analysed CH_m^+ (m/q 12 to 17) region in the H^+ coincidence (Figure 8). It is observed that masses $m/q=12, 13$ and 14 (C^+ , CH^+ , CH_2^+) are clearly visible, but a few counts at m/q 15 (CH_3^+) are present due to chance coincidence with H^+ . This once more supports our argument that production of H^+ , C^+ , CH^+ , and CH_2^+ are related, whereas CH_3^+ is produced exclusively by a different mechanism.

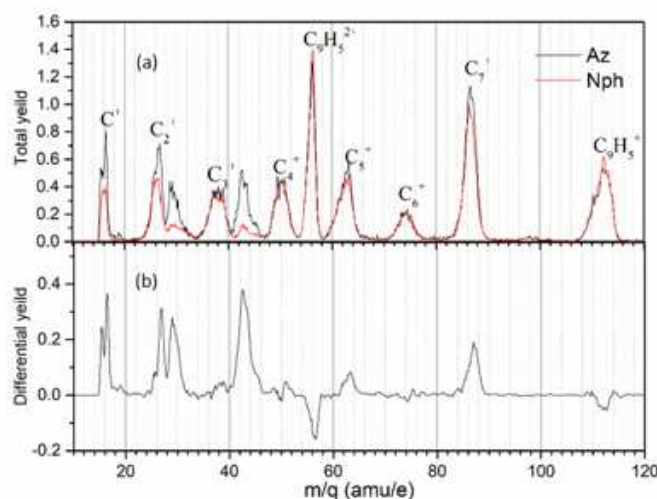


Figure 7. (a) second hit mass spectra of az and nph in coincidence with CH_3^+ ions, (b) the differential second hit mass spectrum between the two isomers for CH_3^+ loss channel .

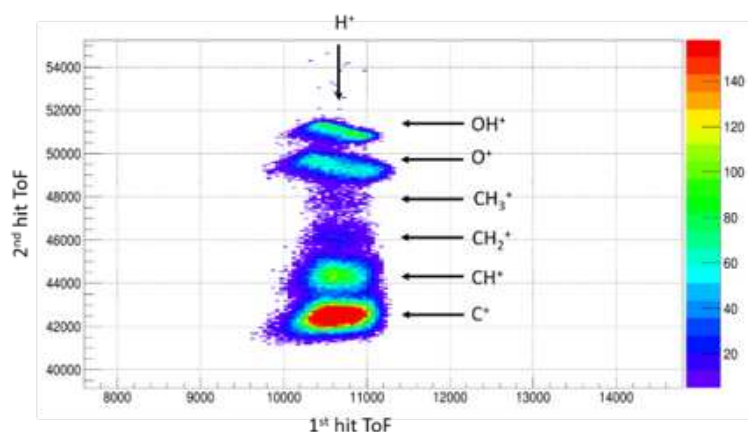



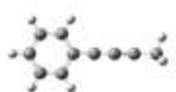


Figure 8. H^+ coincidence with $m/q = 12$ to 17 region. $M/q = 15$ region is filled with only chance coincidence.

CH_3^+ loss from nph/az dication has been studied by a few groups in the past. In this respect, [Kingston et al.](#) proposed structure A (see Table 1) as the originator of $\text{CH}_3^+ + \text{C}_9\text{H}_5^+$ channel. This was further investigated by [Leach et al.](#) to explain the CD^{3+} elimination in nph- d_8 dication on the basis of kinetic energy release (KER)[19]. The experimental KER reported by them was approximately 1 eV, whereas the structure A would correspond to about 2 eV KER and hence [Leach et al.](#) considered a linear geometry, which can be probable over structure A. Our KER measurements for both nph and az target for $\text{CH}_3^+ + \text{C}_9\text{H}_5^+$ channel was found to be 2.9 eV. This value matches very well with the value measured recently by [Reitsma et al.](#). It suggests that a common isomer of az and nph, from which CH_3^+ elimination can occur, might be structure A, as first proposed by [Kingston et al.](#). But, when we performed DFT calculations for other possible structures we observed that the dication structure A was about 3 eV higher in the energy with respect to nph^{2+} . On the other hand, the structure B shown in Table 1 is found to be more favourable with an energy of 2.0 eV more than nph^{2+} . Hence, we propose that the elimination of CH_3^+ might occur via a common dication conformer with structure B. Obviously, the exact transition of nph or az to the parent isomer of CH_3^+ loss channel would occur through various complex intermediate as well as transition states. Such calculations have been carried out for some important channels of monocations but rarely attempted for di or tri cations of nph and az. Calculations of such complexity are presently beyond the scope of this work. But it does not impede the present work in explaining the CH_3^+ elimination in az^{2+} and nph^{2+} via a common isomer,

because the formation of dication in the high energy proton collision proceeds via double plasmon excitation process as suggested in our previous work[12]. This process is found to deposit internal energy of about 13 eV in the resulting dication. Thus, this internal energy will be sufficient to cross any possible transition state barrier the species may encounter on the way to producing CH_3^+ eliminating parent structure. Though the exact formation process of trication is not known as yet, it can be assumed that a similar amount of internal energy can be available for the trications at the time of formation. In addition, we propose the same structure for the possible trication species due to its energy.

Table 1. Energy of C_{10}H_8 isomers in doubly and triply charge state w. r. t. low energy structure, nph (ΔE) . Calculations are done in DFT method at 631G (d) basis.

	Structure	ΔE for dication(eV)	ΔE for trication(eV)
Nph		0	0
Az		0.41	0.29
A		3.07	2.20
B		1.96	1.14

4.7. Multihit analysis in coincidence with CH_3^+

A ToF correlation between second and third hit fragments of C^+ and CH_3^+ channels are shown in Figure 9. While several broad islands are observed in the correlation map of C^+ channel, only three binary dissociation channels of $\text{C}_9\text{H}_5^{2+}$ are observed in case of CH_3^+ emission, which are summarized below.

$$\text{C}_9\text{H}_5^{2+} \Rightarrow \text{C}_n\text{H}_m^+ + \text{C}_{9-n}\text{H}_{m-5}^+ + (5 - m - n)\text{H}$$

(2)

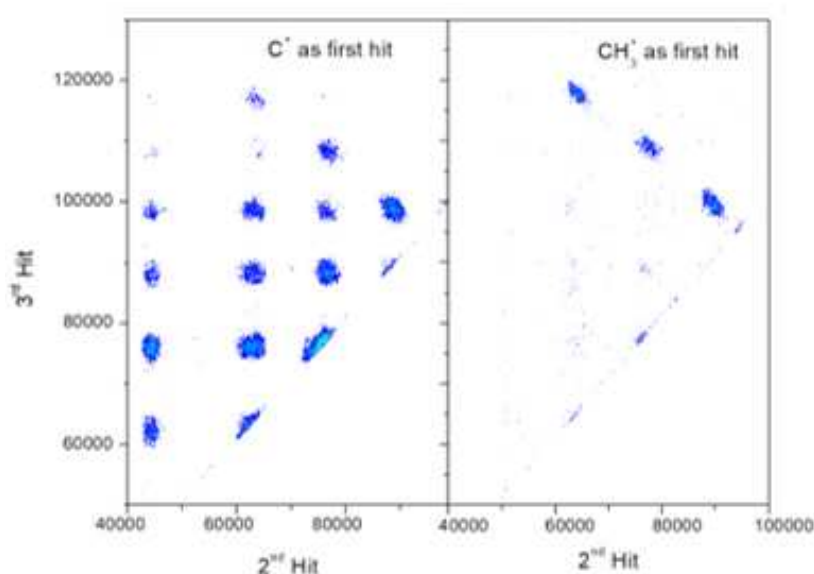


Figure 9. 2nd hit mass spectra of az and nph in coincidence with C^+

The third hit mass spectra of az and nph obtained with CH_3^+ as the first hit are shown in Figure 10. The two mass spectra are very similar and the most prominent channel is the dissociation into $n=4$ and 5 fragments. The formation of such moderate size carbon clusters are of importance in astronomical context [32]. For instance, the structural conformation of partially hydrogenated C_7 and C_9 neutrals as well as ions are proposed as the possible carriers of some weak diffuse interstellar bands (DIBs) in the ISM [33,34]. Steglich et al. calculated the most stable structures of C_9H_5 radicals and also recorded their emission bands to identify the possible carriers of these weak bands. There were seven isomers of C_9H_5 neutral radical, which were proposed as the possible carriers of DIBs in ISM. We consider here the same set of structures for mono- and dications of C_9H_5 .

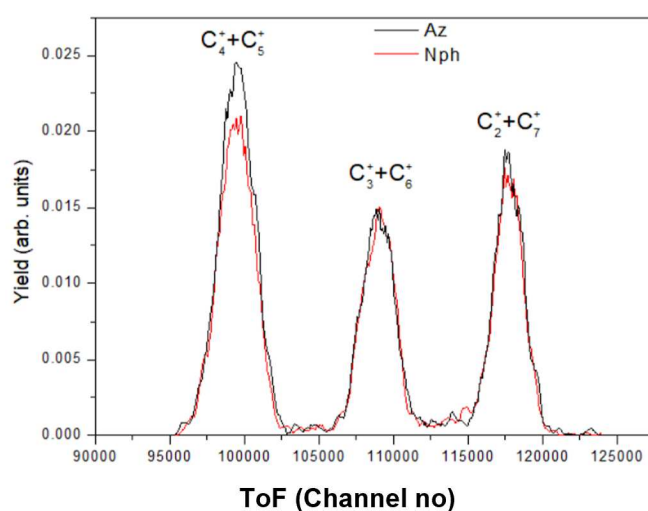
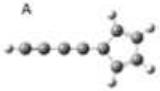
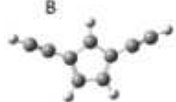

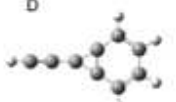

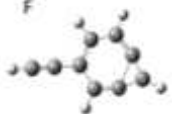
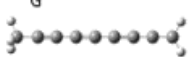


Figure 10. 2nd hit mass spectra of az and nph in coincidence with C^+

The proposed isomers for $C_9H_5^+$ and $C_9H_{52}^+$ fragments are given in Table 2. Their relative ground state energy (a.u.), calculated using DFT is also listed in Table 2. As per this calculation the most stable isomer of $C_9H_{52}^+$ is structure A. It is supported by the mass distribution in the third hit spectrum. We expect to produce a structure of $C_9H_{52}^+$, which can produce C_2 - C_7 , C_3 - C_6 and C_4 - C_5 fragments in equal intensities in the subsequent dissociation. Energetically, structure A and E are good choices for

$C_9H_{52}^+$. But, structure A is most adequate to get observed fragment intensities. The original fragment structure after CH_3^+ elimination may isomerise to structure A. As mentioned earlier, the di- and tri-cations are produced at high internal energies in fast proton collisions. A considerable amount of this internal energy will be utilised in bond dissociation. Therefore, the fragments carry less total internal energy compared to the internal energy available with the parent ion before dissociation. As the fragments separate, the larger fragments are produced closer to the final equilibrium configuration as compared to smaller fragments. The former will therefore be produced at lower temperature than the former. Thus the $C_9H_5^{2+}$ fragment will carry relatively low internal energy per degree of freedom. This implies that in spite of structure E being energetically very close to structure A, $C_9H_5^{2+}$ fragment will prefer structure A. In addition to the dication structure, we have optimised these seven structures to identify stable isomer of $C_9H_5^+$ as well. As per this calculation energetically stable isomer of $C_9H_5^+$ will be structure D.

Table 2. Energy values ((ΔE)) of $C_9H_5^+$ and $C_9H_{52}^+$ isomers w. r. t. lowest energy structure. Calculations are done in DFT method at 631G (d) basis.

Structure	ΔE for monocation(eV)	ΔE for dication(eV)
<div>A</div> 	0.9	0
<div>B</div> 	1.11	0.45
<div>C</div> 	1.33	0.52
<div>D</div> 	0	0.49
<div>E</div> 	0.27	0.02
<div>F</div> 	0.22	1.17
<div>G</div> 	1.54	0.2

5. Conclusions

Swift charged particle induced single and double ionisation of nph as well as az are known to be plasmon dominated. These multiple ionisation processes deposit a high amount of excess energy in the resultant cations, which then can be considered to have high probability of high energy isomer

formation, often followed by dissociation. One such mechanism of CH_3^+ elimination is found to progress via a common isomer of nph and az. Moreover, a cascade of statistical decay is observed in multi hit analysis up to third hit for the same channel. New parent dication as well as trication isomers of nph and az are proposed here with the help of DFT calculations, which can eliminate CH_3^+ . The C_9H_5^+ formed in dication decay of both the molecules was found to further eliminate C_2H_2 to form C_7H_3^+ . The fragment $\text{C}_9\text{H}_{52}^+$ is found to undergo a binary fragmentation process with a clear momentum correlation. The presence of C_4^+ fragments indicated possible $\text{C}_9\text{H}_{52}^+$ structure with a long carbon chain. Various DFT optimised structural conformers were compared and the lowest energy dication structure of $\text{C}_9\text{H}_{52}^+$ was found to have a pentagon and a long linear chain structure. This observation compares favourably with the experimental 3rd hit spectra in coincidence with CH_3^+ as the first hit.

In addition to the decay cascade of CH_3^+ loss channel, a few other observations are also worthy to note. First, we report a process of super-dehydrogenation of PAHs in single collision condition with a detectable intensity of total dehydrogenation for nph and az. Second, the production of H^+ , C^+ , CH^+ , and CH_2^+ are related, whereas CH_3^+ is produced exclusively by a different mechanism. These observations warrant more theoretical as well as experimental investigations.

Author Contributions: Conceptualization, U.K.; methodology, U.K., P.B., C.P. and S.V.; validation, M. V., U.K., C.P. and S.V.; formal analysis, M.V.; investigation, M.V., U.K.; resources, U.K., C.P.; data curation, M.V., U.K.; writing and original draft preparation, M.V., U.K.; writing and review and editing, M.V., U.K., C.P. and S.V.; visualization, M.V., U.K.; supervision, U.K.; project administration, U.K.; All authors have read and agreed to the published version of the manuscript.

Funding: This research received no external funding.

Institutional Review Board Statement: Not applicable.

Informed Consent Statement: Not applicable.

Conflicts of Interest: The authors declare no conflict of interest.

References

1. Van Brunt, R.J.; Wacks, M.E. Electron-Impact Studies of Aromatic Hydrocarbons. III. Azulene and Naphthalene. *The Journal of Chemical Physics* **1964**, *41*, 3195–3199.
2. Ruehl, E.; Price, S.D.; Leach, S. Single and double photoionization processes in naphthalene between 8 and 35 eV. *The Journal of Physical Chemistry* **1989**, *93*, 6312–6321.
3. Jochims, H.; Rasekh, H.; Rühl, E.; Baumgärtel, H.; Leach, S. The photofragmentation of naphthalene and azulene monocations in the energy range 7–22 eV. *Chemical physics* **1992**, *168*, 159–184.
4. Jochims, H.; Baumgärtel, H.; Leach, S. Structure-dependent photostability of polycyclic aromatic hydrocarbon cations: Laboratory studies and astrophysical implications. *The astrophysical journal* **1999**, *512*, 500.
5. Seitz, F.; Holm, A.I.; Zettergren, H.; Johansson, H.A.; Rosén, S.; Schmidt, H.T.; Ławicki, A.; Rangama, J.; Rousseau, P.; Capron, M.; et al. Polycyclic aromatic hydrocarbon-isomer fragmentation pathways: Case study for pyrene and fluoranthene molecules and clusters. *The Journal of chemical physics* **2011**, *135*, 064302.
6. Ławicki, A.; Holm, A.I.; Rousseau, P.; Capron, M.; Maisonnay, R.; Maclot, S.; Seitz, F.; Johansson, H.A.; Rosén, S.; Schmidt, H.T.; et al. Multiple ionization and fragmentation of isolated pyrene and coronene molecules in collision with ions. *Physical Review A* **2011**, *83*, 022704.
7. West, B.; Joblin, C.; Blanchet, V.; Bodi, A.; Sztáray, B.; Mayer, P.M. On the dissociation of the naphthalene radical cation: new iPEPICO and tandem mass spectrometry results. *The Journal of Physical Chemistry A* **2012**, *116*, 10999–11007.
8. Reitsma, G.; Zettergren, H.; Martin, S.; Brédy, R.; Chen, L.; Bernard, J.; Hoekstra, R.; Schlathölter, T. Activation energies for fragmentation channels of anthracene dications—experiment and theory. *Journal of Physics B: Atomic, Molecular and Optical Physics* **2012**, *45*, 215201.
9. Postma, J.; Bari, S.; Hoekstra, R.; Tielens, A.; Schlathölter, T. Ionization and Fragmentation of Anthracene upon Interaction with keV Protons and α Particles. *The Astrophysical Journal* **2009**, *708*, 435.

10. West, B.; Castillo, S.R.; Sit, A.; Mohamad, S.; Lowe, B.; Joblin, C.; Bodi, A.; Mayer, P.M. Unimolecular reaction energies for polycyclic aromatic hydrocarbon ions. *Physical Chemistry Chemical Physics* **2018**, *20*, 7195–7205.
11. Simon, A.; Champeaux, J.P.; Rapacioli, M.; Moretto Capelle, P.; Gadéa, F.X.; Sence, M. Dissociation of polycyclic aromatic hydrocarbons at high energy: MD/DFTB simulations versus collision experiments: Fragmentation paths, energy distribution and internal conversion: test on the pyrene cation. *Theoretical Chemistry Accounts* **2018**, *137*, 1–11.
12. Vinitha, M.; Najeeb, P.; Kala, A.; Bhatt, P.; Safvan, C.; Vig, S.; Kadhane, U. Plasmon excitation and subsequent isomerization dynamics in naphthalene and azulene under fast proton interaction. *The Journal of Chemical Physics* **2018**, *149*, 194303.
13. Bagdia, C.; Biswas, S.; Mandal, A.; Bhattacharjee, S.; Tribedi, L.C. Ionization and fragmentation of fluorene upon 250 keV proton impact. *The European Physical Journal D* **2021**, *75*, 1–7.
14. Leach, S. The formation and destruction of doubly-charged polycyclic aromatic hydrocarbon cations in the interstellar medium. *Journal of electron spectroscopy and related phenomena* **1986**, *41*, 427–438.
15. Witt, A.N.; Gordon, K.D.; Vijh, U.P.; Sell, P.H.; Smith, T.L.; Xie, R.H. The excitation of extended red emission: New constraints on its carrier from hubble space telescope observations of NGC 7023. *The Astrophysical Journal* **2006**, *636*, 303.
16. Mallocci, G.; Joblin, C.; Mulas, G. Theoretical evaluation of PAH dication properties. *Astronomy & Astrophysics* **2007**, *462*, 627–635.
17. Monfredini, T.; Quitián-Lara, H.M.; Fantuzzi, F.; Wolff, W.; Mendoza, E.; Lago, A.F.; Sales, D.A.; Pastoriza, M.G.; Boechat-Roberty, H.M. Destruction and multiple ionization of PAHs by X-rays in circumnuclear regions of AGNs. *Monthly Notices of the Royal Astronomical Society* **2019**, *488*, 451–469.
18. Leach, S.; Eland, J.; Price, S. Formation and dissociation of dications of naphthalene, azulene and related heterocyclic compounds. *The Journal of Physical Chemistry* **1989**, *93*, 7575–7583.
19. Leach, S.; Eland, J.; Price, S. Formation and dissociation of dications of naphthalene-d8. *The Journal of Physical Chemistry* **1989**, *93*, 7583–7593.
20. Sittler, E.C.; Hartle, R.; Bertucci, C.; Coates, A.; Cravens, T.; Dandouras, I.; Shemansky, D. Energy deposition processes in Titan's upper atmosphere and its induced magnetosphere. *Titan from Cassini-Huygens* **2010**, pp. 393–453.
21. Smith, H.; Mitchell, D.; Johnson, R.; Paranicas, C. Investigation of energetic proton penetration in Titan's atmosphere using the Cassini INCA instrument. *Planetary and Space Science* **2009**, *57*, 1538–1546.
22. Sillanpää, I.; Johnson, R.E. The role of ion-neutral collisions in Titan's magnetospheric interaction. *Planetary and Space Science* **2015**, *108*, 73–86.
23. Cravens, T.; Robertson, I.; Ledvina, S.; Mitchell, D.; Krimigis, S.; Waite Jr, J. Energetic ion precipitation at Titan. *Geophysical Research Letters* **2008**, *35*.
24. Gaussian09, R.A. 1, mj frisch, gw trucks, hb schlegel, ge scuseria, ma robb, jr cheeseman, g. Scalmani, v. Barone, b. Mennucci, ga petersson et al., gaussian. Inc., Wallingford CT **2009**, *121*, 150–166.
25. Santos, J.C.; Fantuzzi, F.; Quitián-Lara, H.M.; Martins-Franco, Y.; Menéndez-Delmestre, K.; Boechat-Roberty, H.M.; Oliveira, R.R. Multiply charged naphthalene and its C₁₀H₈ isomers: bonding, spectroscopy, and implications in AGN environments. *Monthly Notices of the Royal Astronomical Society* **2022**, *512*, 4669–4682.
26. Champeaux, J.P.; Moretto-Capelle, P.; Cafarelli, P.; Deville, C.; Sence, M.; Casta, R. Is the dissociation of coronene in stellar winds a source of molecular hydrogen? application to the HD 44179 nebula. *Monthly Notices of the Royal Astronomical Society* **2014**, *441*, 1479–1487.
27. Martínez, J.I.; Alonso, J.A. Hydrogen quenches the size effects in carbon clusters. *Physical Chemistry Chemical Physics* **2019**, *21*, 10402–10410.
28. Wang, H.; Frenklach, M. Calculations of rate coefficients for the chemically activated reactions of acetylene with vinylic and aromatic radicals. *The Journal of Physical Chemistry* **1994**, *98*, 11465–11489.
29. Zhao, L.; Kaiser, R.I.; Lu, W.; Xu, B.; Ahmed, M.; Morozov, A.N.; Mebel, A.M.; Howlander, A.H.; Wnuk, S.F. Molecular mass growth through ring expansion in polycyclic aromatic hydrocarbons via radical–radical reactions. *Nature communications* **2019**, *10*, 3689.
30. Kingston, R.; Guilhaus, M.; Brenton, A.; Beynon, J. Multiple ionization, charge separation and charge stripping reactions involving polycyclic aromatic compounds. *Organic mass spectrometry* **1985**, *20*, 406–412.

31. Reitsma, G.; Zettergren, H.; Boschman, L.; Bodewits, E.; Hoekstra, R.; Schlathölter, T. Ion–polycyclic aromatic hydrocarbon collisions: kinetic energy releases for specific fragmentation channels. *Journal of Physics B: Atomic, Molecular and Optical Physics* **2013**, *46*, 245201.
32. Huang, J.; Oka, T. Constraining the size of the carrier of the $\lambda 5797$. 1 diffuse interstellar band. *Molecular Physics* **2015**, *113*, 2159–2168.
33. Steglich, M.; Maity, S.; Maier, J.P. Visible absorptions of potential diffuse ISM hydrocarbons: C₉H₉ and C₉H₅ radicals. *The Astrophysical Journal* **2016**, *830*, 145.
34. Maity, S.; Steglich, M.; Maier, J.P. Gas Phase Detection of Benzocyclopropenyl. *The Journal of Physical Chemistry A* **2015**, *119*, 10849–10853.

Disclaimer/Publisher's Note: The statements, opinions and data contained in all publications are solely those of the individual author(s) and contributor(s) and not of MDPI and/or the editor(s). MDPI and/or the editor(s) disclaim responsibility for any injury to people or property resulting from any ideas, methods, instructions or products referred to in the content.